Supporting Information

Activating Hematite Nanoplates *via* Partial Reduction for Electrocatalytic Oxygen Reduction Reaction

Hao Wan,[ab] Menghua Lv,[b] Xiaohe Liu,[a] Gen Chen,[a] Ning Zhang,[a] Yijun Cao,[c] Haidong Wang,*[b] Renzhi Ma,*[d] Guanzhou Qiu[b]*

[a] State Key Laboratory of Powder Metallurgy and School of Materials Science and Engineering, Central South University, No. 932 South Lushan Road, Changsha, Hunan 410083, P.R. China. Email: liuxh@csu.edu.cn

[b] School of Resources Processing and Bioengineering, Central South University, No. 932 South Lushan Road, Changsha, Hunan 410083, P.R. China. E-mail: joew@csu.edu.cn

[c] Henan Province Industrial Technology Research Institute of Resources and Materials, Zhengzhou University, No. 100 Science Avenue, Zhengzhou, Henan 450001, P. R. China.

[d] International Center for Materials Nanoarchitectonics (WPI-MANA), National Institute for Materials Science (NIMS), Namiki 1-1, Tsukuba, Ibaraki 305-0044, Japan. Email: MA.Renzhi@nims.go.jp

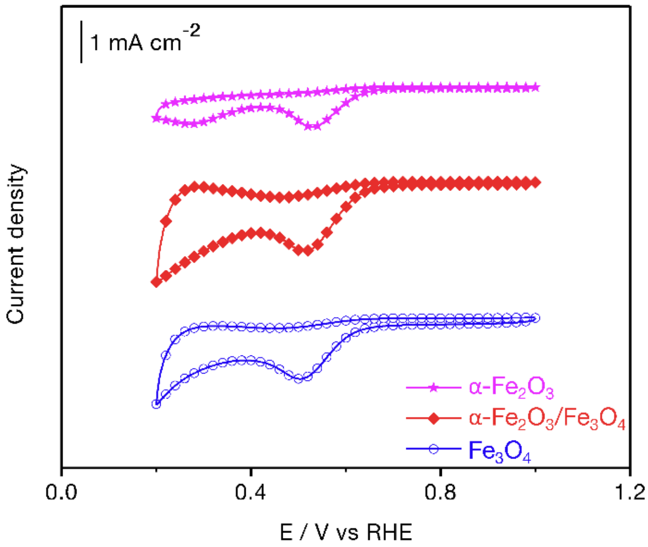

Figure S1. CV curves of α-Fe_2O_3, α-Fe_2O_3/Fe_3O_4, Fe_3O_4 products. Here, α-Fe_2O_3/Fe_3O_4 composite corresponds to Sample-1h.

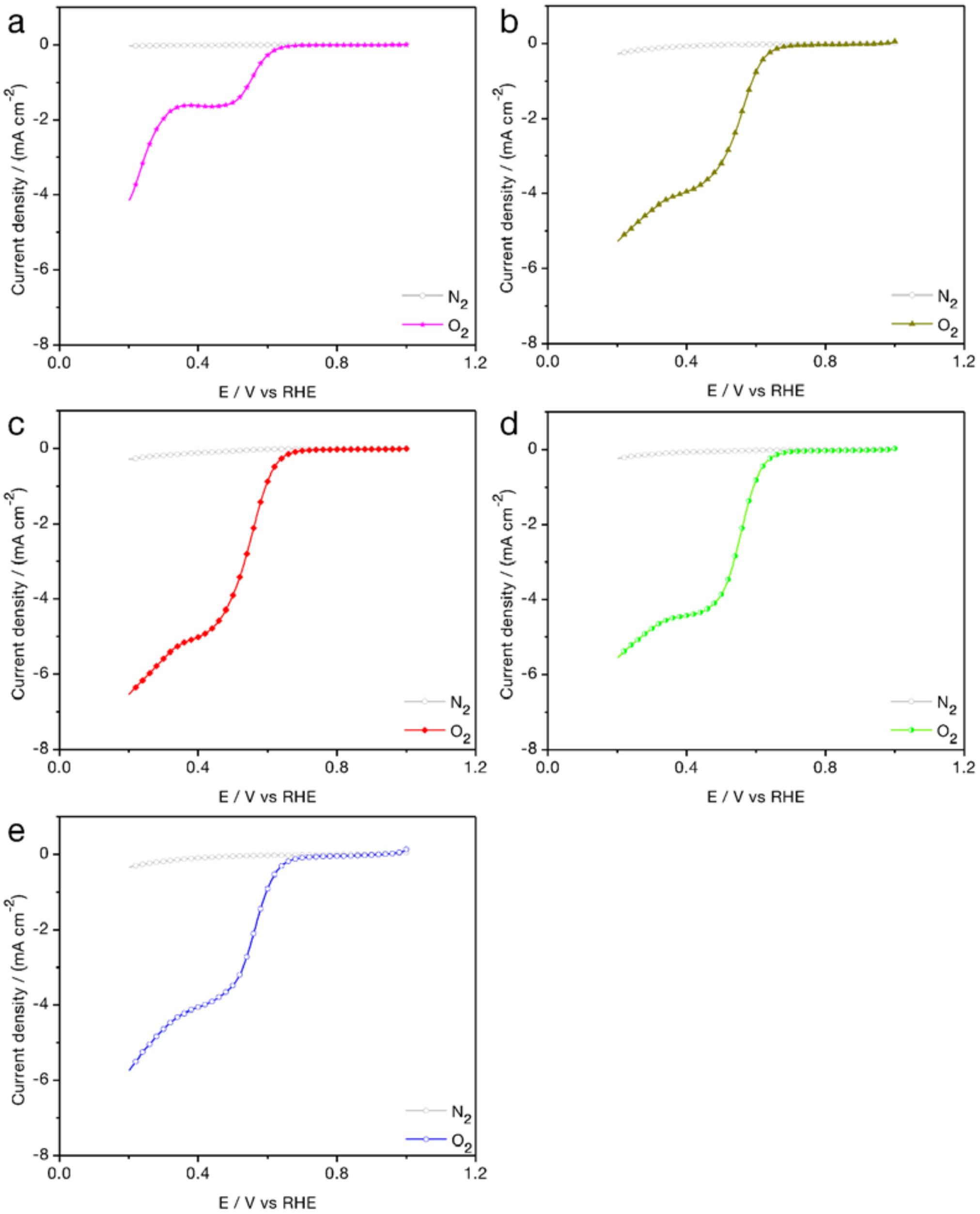

Figure S2. Polarization curves in N_2- or O_2-saturated KOH electrolyte. (a) α-Fe_2O_3 nanoplates, (b) Sample-0.5h, (c) Sample-1h, (d) Sample-3h and (e) Sample-10h.

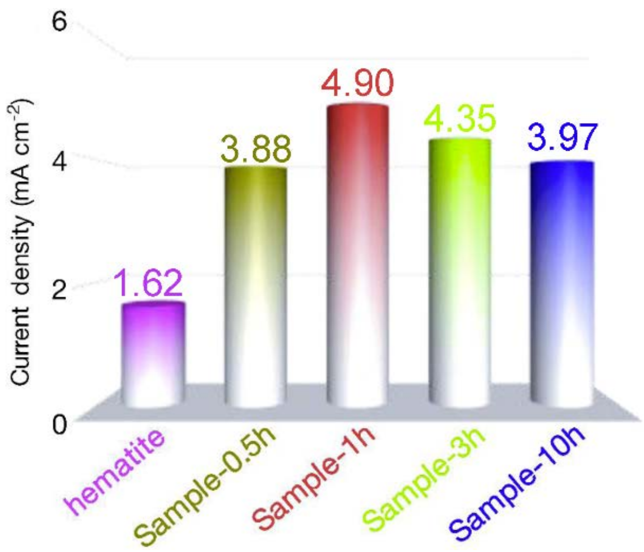

Figure S3. The current densities achieved by the as-prepared electrocatalysts at the potential of 0.4 V vs RHE.

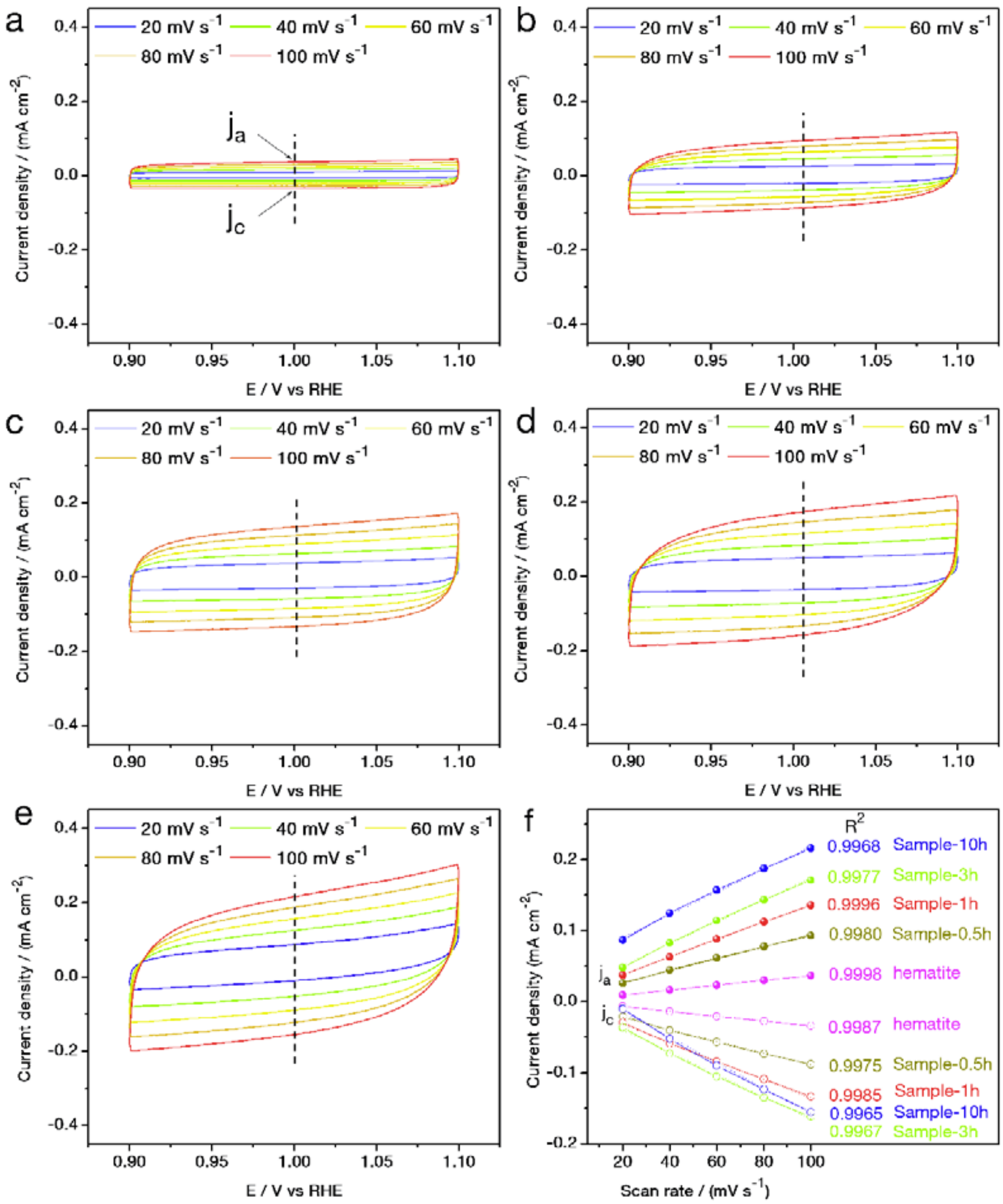

Figure S4. CV curves of (a) α-Fe_2O_3 nanoplates, (b) Sample-0.5h, (c) Sample-1h, (d) Sample-3h and (e) Sample-10h at different scan rates. (f) Anodic and cathodic current densities (denoted as j_a and j_c, respectively) of iron oxide samples at the potential of 1.0 V vs RHE as a function of the scan rate. It can be seen that there exists a highly standard linear relationship between the current density and scan rate with all the coefficient of determinations (R^2) over 0.9965 close to 1, revealing that in such a potential region, all of the iron oxides almost act as an ideal double-layer capacitor.

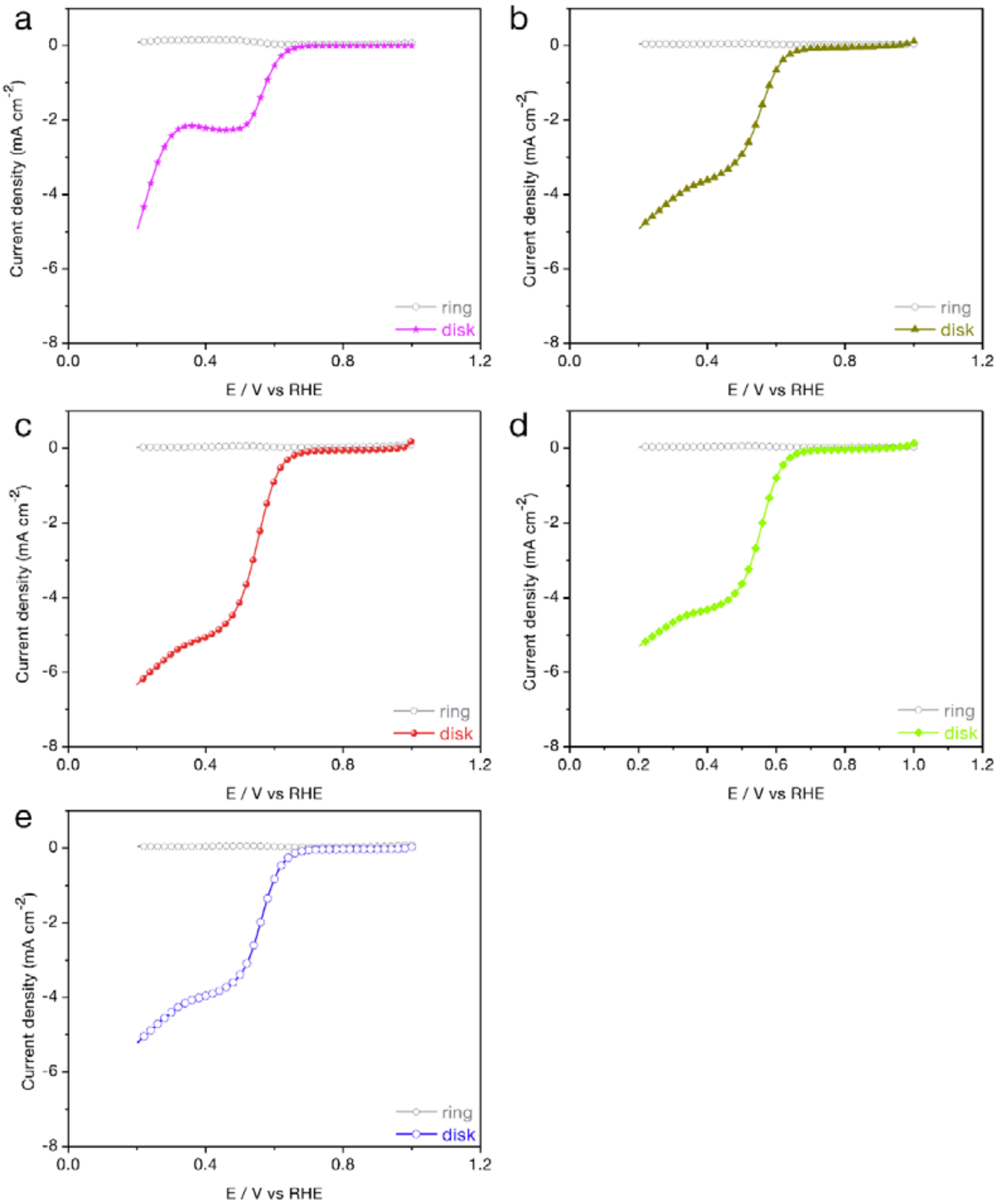

Figure S5. Polarization curves tested using RRDE method. (a) α-Fe_2O_3 nanoplates, (b) Sample-0.5h, (c) Sample-1h, (d) Sample-3h and (e) Sample-10h.

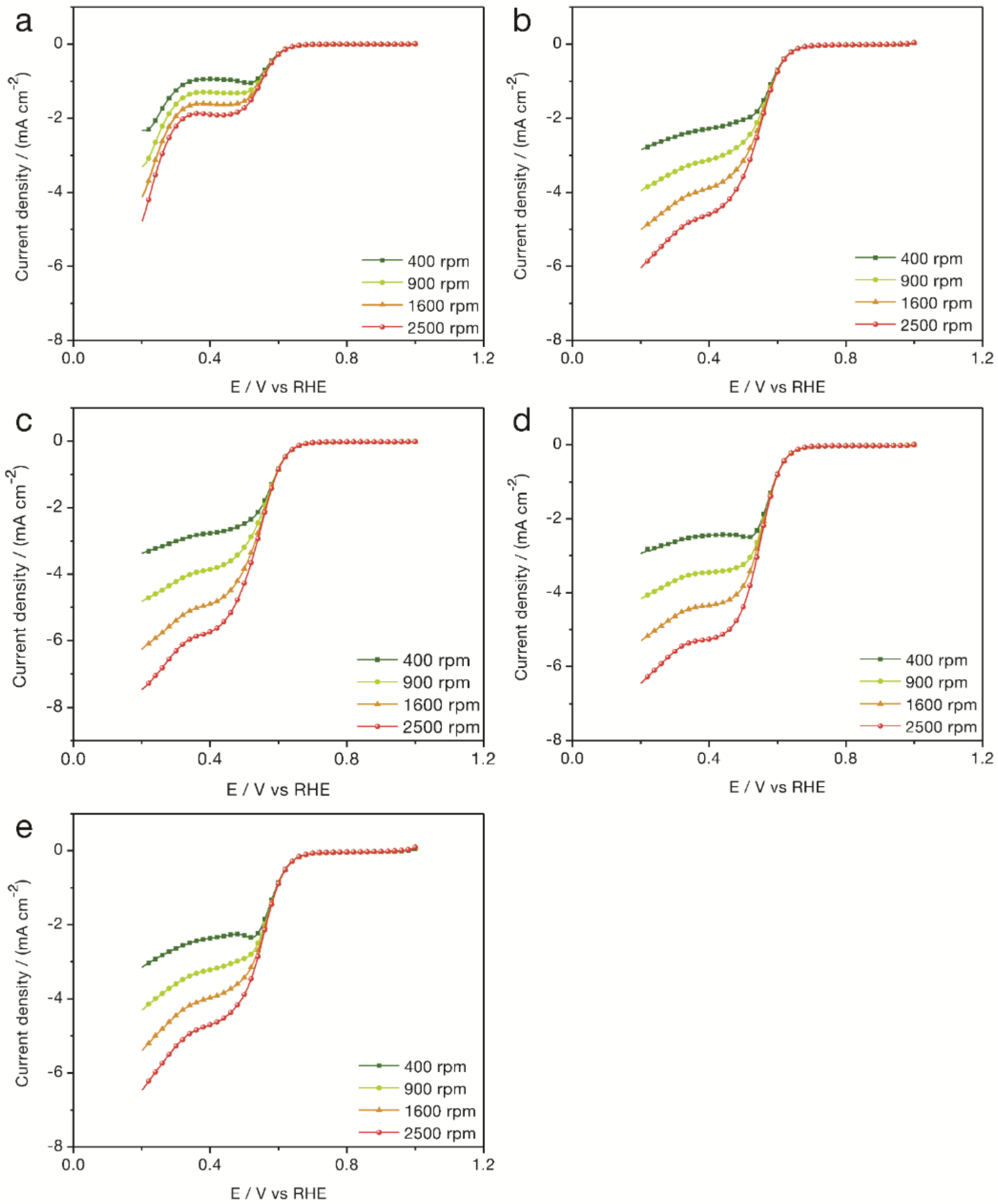

Figure S6. Polarization curves of as-prepared iron oxides tested at different rotating rates. (a) α-Fe_2O_3 nanoplates, (b) Sample-0.5h, (c) Sample-1h, (d) Sample-3h and (e) Sample-10h.

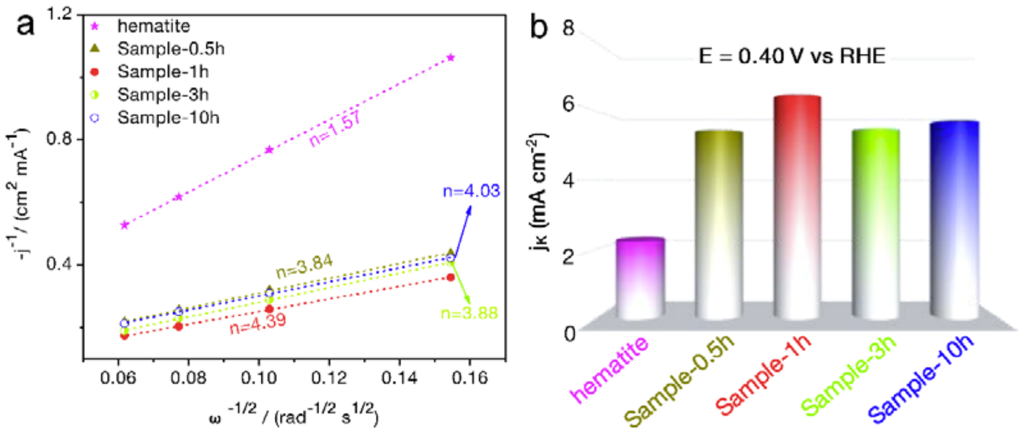

Figure S7. (a) Calculated electron transfer number using K-L method and (b) j_K of as-prepared iron oxide materials. Electron transfer number was estimated as 1.57, 3.84, 4.39, 3.88 and 4.03 for α-Fe_2O_3 nanoplates, Sample-0.5h, Sample-1h, Sample-3h and Sample-10h, respectively.

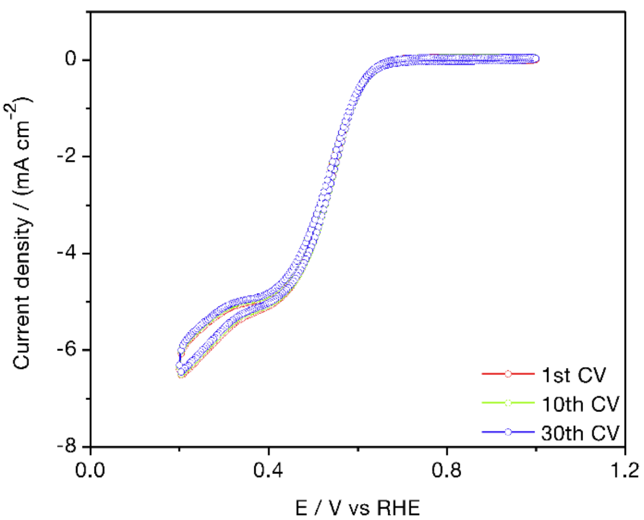

Figure S8. The 1st, 10th and 30th CV curves of Sample-1h.

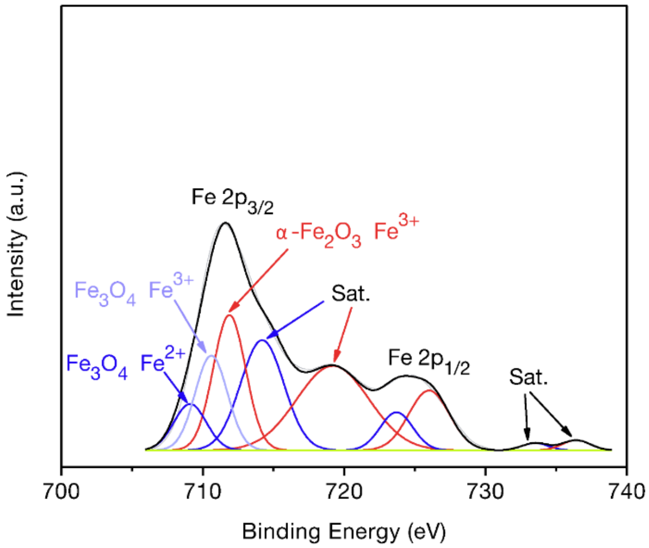

Figure S9. Fe 2p region of Sample-1h after a chronoamperometry measurement at 0.60 V vs RHE for 800 s.

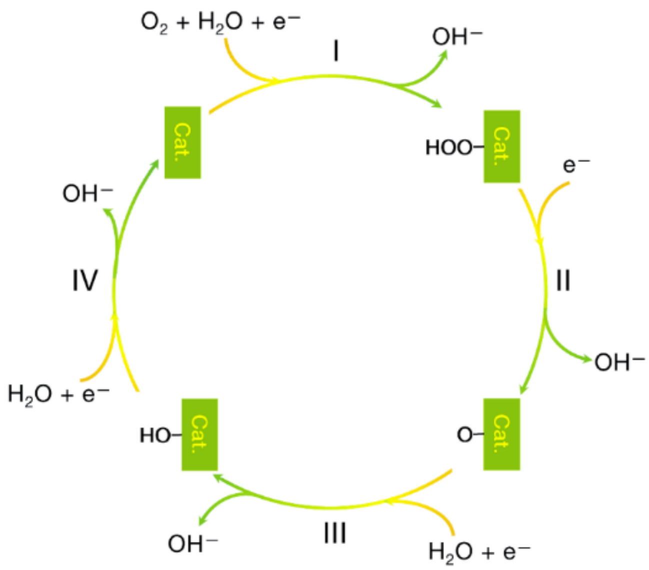

Figure S10. Electrocatalytic oxygen reduction process of 4-electron pathway.

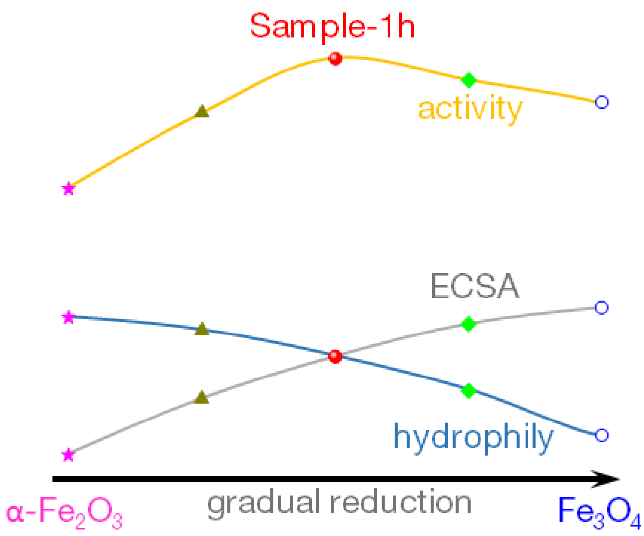

Figure S11. Plausible mechanism for the best performance of Sample-10h.

Table S1. Activity comparison of iron oxide materials for electrocatalytic oxygen reduction process in 0.1 M KOH electrolyte.

Materials	j (mA cm^{-2}) @ 0.4 V vs RHE	Tafel slope (mV dec^{-1})	Electron transfer number	Ref.
α-Fe_2O_3	1.62	107	3.19 @ 0.4 V vs RHE	
Sample-0.5h	3.88	89	3.81 @ 0.4 V vs RHE	
Sample-1h	4.90	76	3.89 @ 0.4 V vs RHE	this work
Sample-3h	4.35	81	3.85 @ 0.4 V vs RHE	
Sample-10h	3.97	86	3.83@ 0.4 V vs RHE	
α-Fe_2O_3/CNTs	3.72	–	3.45 @ 0.365 V vs RHE	S1
α-Fe_2O_3/Ppy/GO	1.23	–	3.91 @ 0.4 V vs RHE	S2
α-Fe_2O_3/N-doped CNTs	3.82	–	3.37 @ 0.365 V vs RHE	S3

Table S2. Fitting parameters of the electronic components in the equivalent circuit as shown in the inset of Figure 6c.

Materials	R_0 (Ω)	R_1 (Ω)	R_2 (Ω)
α-Fe_2O_3	66.73	626.8	290.7
Sample-0.5h	70.85	455.6	141.7
Sample-1h	64.44	325.6	140.4
Sample-10h	64.66	392.5	132.2
Sample-10h	65.22	450.8	140.5

References

(S1) Sun, M.; Dong, Y.; Zhang, G.; Qu, L.; Li, J. α-Fe_2O_3 spherical nanocrystals supported on CNTs as efficient non-noble electrocatalysts for the oxygen reduction reaction. *J. Mater. Chem. A* **2014**, *2*(33), 13635–13640, DOI: 10.1039/c4ta02172j.

(S2) Ren, S.; Ma, S.; Yang, Y.; Mao, Q.; Hao, C. Hydrothermal synthesis of Fe_2O_3/polypyrrole/graphene oxide composites as highly efficient electrocatalysts for oxygen reduction reaction in alkaline electrolyte. *Electrochim. Acta* **2015**, *178*, 179–189, DOI: 10.1016/j.electacta.2015.07.181.

(S3) Sun, M.; Zhang, G.; Liu, H.; Liu, Y.; Li, J. α- and γ-Fe_2O_3 nanoparticle/nitrogen doped carbon nanotube catalysts for high-performance oxygen reduction reaction. *Sci. China Mater.* **2015**, *58*(9), 683–692, DOI: 10.1007/s40843-015-0082-x.